# Probabilistic Wind Power Ramp Forecasting Based on a Scenario Generation Method

Mingjian Cui, Cong Feng, Zhenke Wang, Jie Zhang
University of Texas at Dallas
Richardson, TX, 75080 USA

Qin Wang, Anthony Florita, Venkat Krishnan, Bri-Mathias Hodge
National Renewable Energy Laboratory
Golden, CO, 80401 USA

***Abstract*—Wind power ramps (WPRs) are particularly important in the management and dispatch of wind power and currently drawing the attention of balancing authorities. With the aim to reduce the impact of WPRs for power system operations, this paper develops a probabilistic ramp forecasting method based on a large number of simulated scenarios. An ensemble machine learning technique is first adopted to forecast the basic wind power forecasting scenario and calculate the historical forecasting errors. A continuous Gaussian mixture model (GMM) is used to fit the probability distribution function (PDF) of forecasting errors. The cumulative distribution function (CDF) is analytically deduced. The inverse transform method based on Monte Carlo sampling and the CDF is used to generate a massive number of forecasting error scenarios. An optimized swinging door algorithm is adopted to extract all the WPRs from the complete set of wind power forecasting scenarios. The probabilistic forecasting results of ramp duration and start-time are generated based on all scenarios. Numerical simulations on publicly available wind power data show that within a predefined tolerance level, the developed probabilistic wind power ramp forecasting method is able to predict WPRs with a high level of sharpness and accuracy.**

***Index Terms*—Gaussian mixture model, probabilistic wind power ramp forecasting, scenario generation.**

## I. Introduction

Large fluctuations in wind speed in a short time period can cause significant wind power ramps (WPRs) and threaten the power system's reliability [1], [2]. WPRs can generally be divided into up-ramping, down-ramping, or non-ramping periods. This is becoming more challenging for system operators as larger wind power penetrations are seen in power systems worldwide.

A number of statistical and machine learning methods have been developed in the literature to forecast wind power ramps at multiple forecast horizons. Liu *et al*. [3] developed a hybrid forecasting model to combine an orthogonal test with support vector machine. Cutler *et al*. [4] forecasted wind power ramps and evaluated the efficiency of the Wind Power Prediction Tool (WPPT) and the Mesoscale Limited Area Prediction System (MesoLAPS) for ramp forecasting. Greaves *et al*. [5] forecast up-ramps and down-ramps with uncertain start times and incorporated a numerical weather prediction (NWP) model to reduce the forecasting errors. However, most of existing methods focus on the deterministic ramp forecasting. Probabilistic ramp forecasting is expected to provide more information, and thus produce better system schedules for balancing authorities. Taylor [6] used a multinomial logit structure and categorical distribution to estimate the ramp event probabilities for different thresholds. Li *et al*. [7] provided additional probabilistic information for wind ramp occurrences by using a logistic regression technique. This paper seeks to develop a probabilistic wind power ramp forecasting method to characterize different key ramp features.

The organization of this paper is as follows. In Section II, a wind power forecasting scenario generation method using the Guassian mixture model is developed. In Section III, the methodology of probabilistic wind power ramp forecasting is presented. Case studies and results analysis performed on publically available wind power data are discussed in Section IV. Concluding remarks and future work are summarized in Section V.

## II. Wind Power Forecasting and Massive Forecasting Error Scenario Generation

### *A. Basic Forecasting Scenario Generation Using Ensemble Machine Learning Techniques*

Due to the nonlinear and non-stationary characteristics of wind power, it is challenging for a single machine learning algorithm to produce forecasts that are consistently better than all other methods. Ensemble machine learning techniques blend multiple forecasts from individual forecasting algorithms to generate a forecast superior to each individual forecast [8]. In this paper, an ensemble machine learning model is adopted, which integrates four machine learning algorithms: neural networks (NN), support vector machines (SVM), gradient boosting machines (GBM), and random forest regression (RF).

### *B. Forecasting Error Scenario Generation Based on Gaussian Mixture Models*

Historical wind power forecasting errors of the ensemble model are calculated and recorded. A Gaussian mixture model (GMM) is used to fit the distribution of forecasting errors. The GMM is a probabilistic model that assumes all the data points are generated from a mixture of a finite number of Gaussian distributions with multiple parameters. The GMM generally performs better than other specific distributions that follow an asymmetric distribution [9], [10], especially for multi-modal

probability distributions. The generalized GMM is formulated as:

$$f_{\mathrm{G}}(x;\mathrm{N_G};\omega_i,\mu_i,\sigma_i)=\sum_{i=1}^{\mathrm{N_G}}\omega_i g_i(x;\mu_i,\sigma_i)$$
$$=\sum_{i=1}^{\mathrm{N_G}}\omega_i e^{-\left[\frac{x-\mu_i}{\sigma_i}\right]^2},\ \forall x\in\mathscr{X},\ \forall i\in\mathscr{I} \quad (1)$$

where $\mathscr{X}$ is the data set of forecasting errors, $x$, with the total number of $\mathrm{N}_x$. $\mathscr{I}$ is the set of GMMs with the total number of $\mathrm{N_G}$. A two-stage optimization model is constructed to estimate all the parameters of $f_{\mathrm{G}}$, i.e., $\mathrm{N_G}$, $\omega_i$, $\mu_i$, and $\sigma_i$. The first stage aims to determine the expected value (or mean value) vector $\mathrm{M}$ ($\mu_i\in\mathrm{M}$), the standard deviation vector $\Sigma$ ($\sigma_i\in\Sigma$), and the weight coefficient vector $\Omega$ ($\omega_i\in\Omega$), i.e., $f_{\mathrm{G}}(x;\mathrm{N_G};\omega_i,\mu_i,\sigma_i)\rightarrow f_{\mathrm{G}}(x;\mathrm{N_G})$. The non-linear least square method with the Trust-Region algorithm [11] is adopted in the first stage. The second stage aims to determine the optimal number of GMM, $\mathrm{N_{G,opt}}$, by minimizing the Euclidean distance between the actual PDF, $f_{\mathrm{A}}$, and the PDF of GMM, $f_{\mathrm{G}}$, i.e., $f_{\mathrm{G}}(x;\mathrm{N_G})\xrightarrow{\mathrm{N_{G,opt}}}f_{\mathrm{G}}(x)$. The objective function is formulated as:

$$\min\ \sqrt{\sum_{x\in\mathscr{X}}\left[f_{\mathrm{G}}(x;\mathrm{N_G})-f_{\mathrm{A}}\right]^2} \quad (2)$$

The cumulative distribution function (CDF), $F_{\mathrm{G}}$, is essential for sampling due to its monotonicity and can be analytically expressed as:

$$F_{\mathrm{G}}(x;\mathrm{N_G};\omega_i,\mu_i,\sigma_i)=\sum_{i=1}^{\mathrm{N_G}}\left[\frac{\sqrt{\pi}}{2}\omega_i\sigma_i\mathrm{erf}(\frac{\mu_i-x}{\sigma_i})\right]+\mathrm{C} \quad (3)$$

where erf is the Gaussian error function and defined as:

$$\mathrm{erf}(x)=\frac{2}{\sqrt{\pi}}\int_0^x e^{-t^2}dt \quad (4)$$

Equation (3) is an indefinite integral with a constant C that is solved by (5). Since both the actual and forecast wind power are normalized into the range [0, 1], the forecasting errors are distributed into the range [-1, 1]. Thus $F_{\mathrm{G}}(x<-1)=0$ and $F_{\mathrm{G}}(x>1)=1$. In this paper, we use $x=-1.1$ ($F_{\mathrm{G}}(-1.1)=0$) to calculate C, shown as:

$$\mathrm{C}=F_{\mathrm{G}}(-1.1)-\sum_{i=1}^{\mathrm{N_G}}\left[\frac{\sqrt{\pi}}{2}\omega_i\sigma_i\mathrm{erf}(\frac{-1.1-\mu_i}{\sigma_i})\right] \quad (5)$$

To sample a random forecasting error, $\hat{x}$, the inverse transform method that has been widely utilized in the financial engineering literature [12] is adopted in this paper and formulated as:

$$\hat{x}=F_{\mathrm{G}}^{-1}(\int_{-\infty}^{r}\frac{1}{\sqrt{2\pi}\Sigma_{\mathrm{MND}}}e^{-\left[\frac{t-\mu_{\mathrm{MND}}}{\sqrt{2}\Sigma_{\mathrm{MND}}}\right]^2}dt) \quad (6)$$

where $r$ is a random variable uniformly distributed over [0, 1]. $F_{\mathrm{G}}^{-1}$ is the inverse function of $F_{\mathrm{G}}$. $\mu_{\mathrm{MND}}$ and $\Sigma_{\mathrm{MND}}$ are the mean and covariance vectors of the multivariate normal distribution (MND), respectively. In this paper, $\mu_{\mathrm{MND}}$ is defined as a zero $N_{\mathrm{sc}}$-by-$T_{\mathrm{fh}}$ matrix. $N_{\mathrm{sc}}$ is the total number of forecasting error scenarios. $T_{\mathrm{fh}}$ is the maximum forecasting horizon. $\Sigma_{\mathrm{MND}}$ is a $T_{\mathrm{fh}}$-by-$T_{\mathrm{fh}}$ symmetric positive semi-definite matrix with a covariance $\sigma_{n,m}$, which can be modeled by an exponential covariance function [13] and is defined as:

$$\sigma_{n,m}=\mathrm{cov}(r_n,r_m)=e^{-\frac{|n-m|}{\lambda}},\quad 0\le n,m\le T_{\mathrm{fh}} \quad (7)$$

where $\lambda$ is the range parameter that controls the strength of the correlation of random variables $r_n$ and $r_m$.

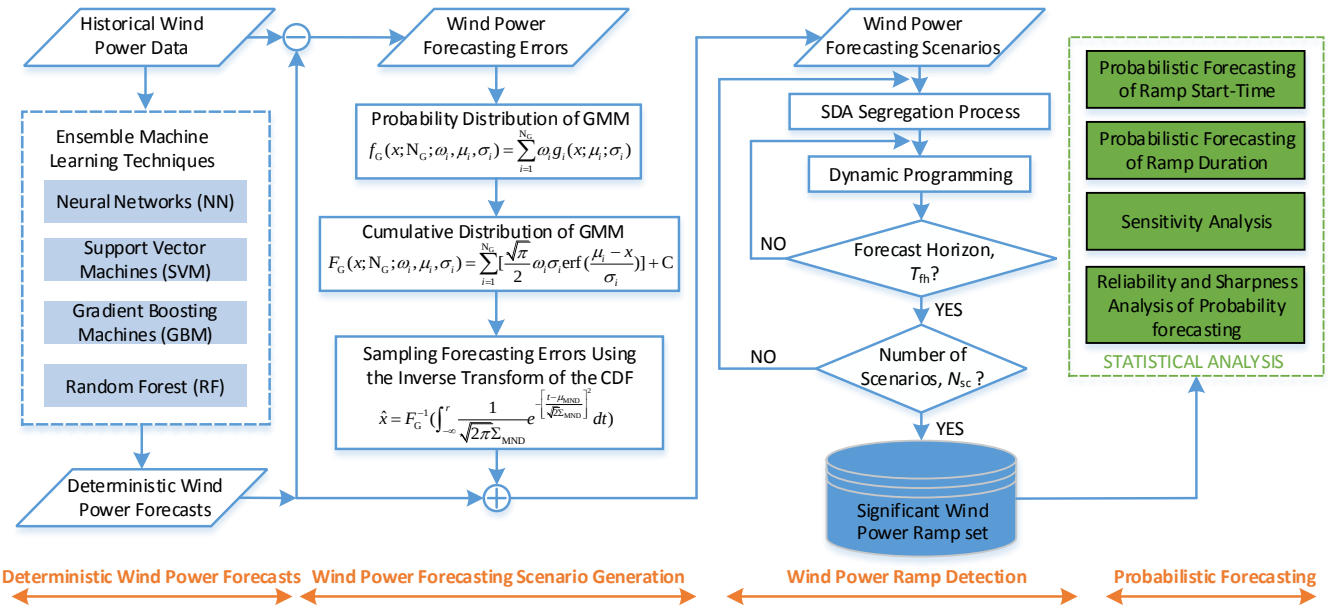


Fig. 1. The overall framework for developing the probabilistic wind power ramp forecasts.

Thus, the forecasting error scenarios are generated by setting a total number of $N_{\rm sc}$, with a specific forecast horizon of $T_{\rm fh}$ (e.g., day-ahead, hours-ahead, or minutes-ahead). A complete set of the wind power forecasting scenarios is obtained by combining the basic ensemble deterministic wind power forecast with all the forecasting error scenarios.

## III. Probabilistic Ramp Forecasting Methodology

### A. Wind Power Ramp Detection Method

Based on the generated wind power forecasting scenarios, an optimized swinging door algorithm (OpSDA) [14] is used to detect all the wind power ramps at each timescale. In the OpSDA, the swinging door algorithm with a predefined parameter, $\varepsilon$, is first applied to segregate the wind power data into multiple discrete segments. Then dynamic programming is used to merge adjacent segments with the same ramp direction and relatively high ramping rates. A brief description of the OpSDA is introduced here, but more details can be found in [14]. Subintervals that satisfy the ramping rules are rewarded by a score function; otherwise, their score is set to zero. The current subinterval is retested as above after being combined with the next subinterval. This process is performed recursively until the end of the dataset. A positive score function, $S$, is designed based on the length of the interval segregated by the swinging door algorithm. Given a time interval $(u,\ v)$ of all discrete time points and an objective function, $J$, of the dynamic programming, a wind power ramp is detected by maximizing the objective function, $J$:

$$J(u,v) = \max_{u<k<v} [S(u,k) + J(k,v)], \quad u < v \tag{8}$$

where $k$ is the time point over the time interval $(u,\ v)$.

### B. Probabilistic Wind Power Ramp Forecasting

Probabilistic wind power ramp forecasts are generated by using a massive number of forecast scenarios, and extracting out their ramps with the wind power ramp detection method. The overall framework for generating probabilistic wind power ramp forecasts is illustrated in Fig. 1, which consists of four major steps: deterministic wind power forecasts, forecasting scenario generation, wind power ramp detection, and probabilistic forecasting and analysis. The four major steps are described as follows:

- ***Step 1***: Based on historical wind power data, an ensemble machine learning method blends the forecasts from four individual machine learning techniques to generate deterministic wind power forecasts.
- ***Step 2***: Historical wind power forecasting errors are generated from the basic ensemble forecasting model. The GMM probability distribution model is adopted to fit the probability distribution of historical wind power forecasting errors and the cumulative distribution of GMM is analytically deduced. The inverse transform method based on Monte Carlo sampling [15] is used to simulate the massive wind power forecasting error scenarios.
- ***Step 3***: A wind power forecasting scenario is generated by adding the basic ensemble forecasting data with each individual forecasting error scenario. A three-dimensional plot with massive wind power forecasting scenarios is illustrated in Fig. 2. Each scenario is put into the OpSDA algorithm to extract all the significant wind power ramps.
- ***Step 4***: The probabilistic wind power ramp forecasts are generated and analyzed, such as the ramp start-time and duration.

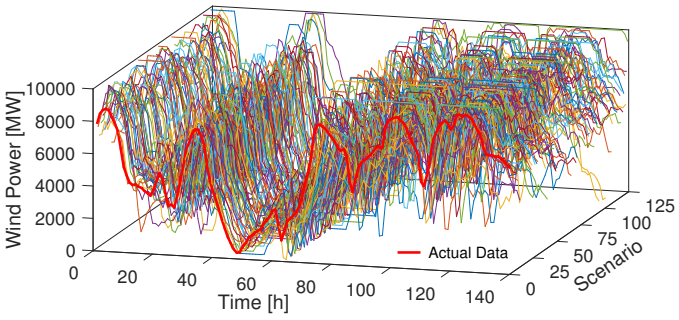


Fig. 2. A three-dimensional plot of one particular timeslice of wind power forecasting scenarios spanning from April 17th to 22nd 2007 near Dallas, Texas, with an hourly data resolution. An example with 125 scenarios is illustrated here.

## IV. Case Studies

### A. Test Case

The developed scenario-based wind power ramp forecasting model was verified using the Wind Integration National Dataset (WIND) Toolkit [16]. The data represent wind power generation from January 1st 2007 to December 31st 2012. The wind plants used in this analysis are from 711 wind sites near Dallas, Texas, with an hourly data resolution. The total rated wind power capacity is 9,987 MW. The training data use historical wind power data recorded from January 1st 2007 to April 16th 2007, with a total of 2,544 hours. The test data use the consecutive data from April 17th 2007 to August 22th 2007, with a total of 3,000 hours. An example of the consecutive test data spanning from April 17th to 22nd 2007 is shown in Fig. 2 for the convenience of visual inspection. The ensemble machine learning model consists of seven Neural Network models, five Support Vector Machine models, four Gradient Boosting Machine models, and two Random Forest models. The door width of the OpSDA is set as 0.2% of the rated capacity. The total number of forecasting scenarios is set as $N_{\rm sc} = 10,000$.

### B. Performance of Different Distribution Models for Wind Power Forecasting Errors

Fig. 3 compares the probability and cumulative distributions of wind power forecasting errors from six distributions. The optimal parameters of weight coefficients, mean values, and standard deviations are listed in Table I. The coefficient of determination, $R^2$, is used to evaluate the correlation between the observed and modeled data values. The Extreme Value distribution has the smallest coefficient of determination, 0.8328, and the GMM distribution shows the largest coefficient of

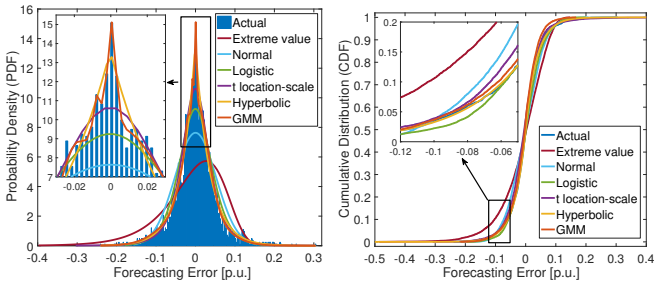


(a) Probability distribution (b) Cumulative distribution

Fig. 3. Probability and cumulative distribution plots for hourly forecasting errors using six distribution models. Extreme Value: $\mu = 0.0267, \sigma = 0.0643$; Normal: $\mu = 1.72 \times 10^{-6}, \sigma = 0.0522$; Logistic: $\mu = -3.09 \times 10^{-4}, \sigma = 0.027$; t Location-Scale Distribution: $\mu = -2.53 \times 10^{-4}, \sigma = 0.0346, \nu = 3.11$; and Hyperbolic: $\pi = 4.72 \times 10^{-3}, \zeta = 2.09 \times 10^{-4}, \delta = 7.69 \times 10^{-6}, \mu = -3.39 \times 10^{-4}$.

TABLE I
PARAMETERS OF GMM WITH FIVE MODELS ($N_{G,opt} = 5$)

| Number of GMMs | $\omega$ | $\mu$ | $\sigma$ |
|---|---|---|---|
| 1 | -5,119 | -0.0031 | 0.0041 |
| 2 | 5,121 | -0.0031 | 0.0041 |
| 3 | 1.1068 | -0.0205 | 0.0065 |
| 4 | 7.1448 | 0.0034 | 0.0404 |
| 5 | 2.5256 | -0.0089 | 0.0944 |

determination, 0.9922. The coefficients of determination of Normal, Logistic, t Location-Scale, and Hyperbolic distributions are 0.9352, 0.9698, 0.9828, and 0.9873, respectively. Both the coefficient of determination and Fig. 3 show that the GMM distribution outperforms other distributions in modeling the wind power forecasting errors.

### C. Probabilistic Forecasting of Ramp Duration

After generating a massive number of wind power forecasting scenarios as shown in Fig. 2, the number of upward and downward ramps occurring within a tolerance value, $\delta$, is calculated and expressed by $N^{\delta}_{\text{up}}$ and $N^{\delta}_{\text{down}}$, respectively. The forecasting probability of the upward and downward ramps within the tolerance value, $\delta$, is represented by $p^{\delta}_{\text{up}}$ and $p^{\delta}_{\text{down}}$, and formulated as $p^{\delta}_{\text{up}} = \Pr(N^{\delta}_{\text{up}}, N_{\text{sc}} \mid \delta) = N^{\delta}_{\text{up}}/N_{\text{sc}}$ and $p^{\delta}_{\text{down}} = \Pr(N^{\delta}_{\text{down}}, N_{\text{sc}} \mid \delta) = N^{\delta}_{\text{down}}/N_{\text{sc}}$, respectively. The probabilities of occurrence forecasts for two different upward and downward WPRs are illustrated in Fig. 4 and Fig. 5, respectively. Three cases with different tolerance values are studied: without tolerance ($\delta$=0), 1-hour tolerance ($\delta$=1), and 2-hour tolerance ($\delta$=2). For each upward or downward ramp, the occurrence probability is calculated within a certain time interval. The probability of WPR occurrence is increased with the tolerance value, as illustrated by the wider banded areas.

The sensitivity results of different tolerance values are illustrated in Fig. 6. It is shown that the probability of wind power ramps increases with the tolerance value. This information can be potentially used by power system operators to determine the probability of wind power ramps based on the corresponding tolerance value. For instance, if the power system operators set the tolerance value as 1 hour, i.e., $\delta$ = 1, the probability of

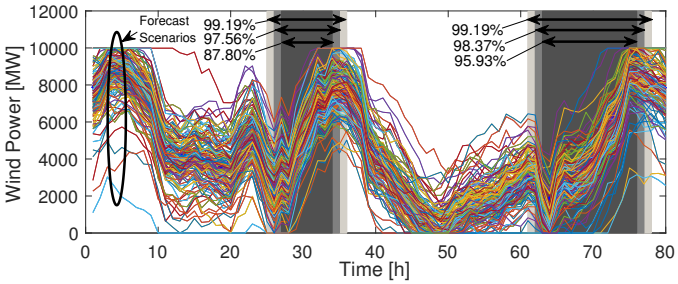


Fig. 4. Upward ramps of probabilistic forecasting of ramping duration with banded areas.

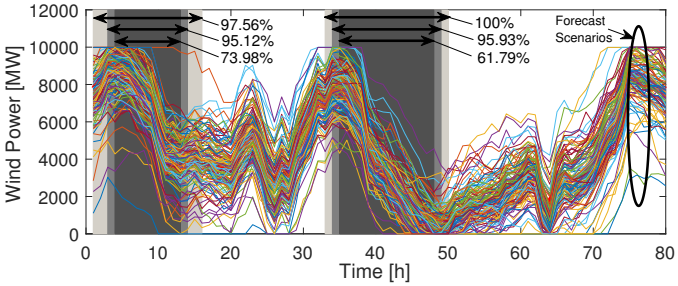


Fig. 5. Downward ramps of probabilistic forecasting of ramping duration with banded areas.

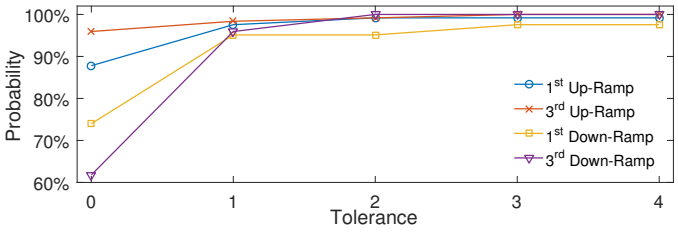


Fig. 6. Sensitivity of wind ramp duration probability to the tolerance value.

correctly forecasting a ramp is larger than 90% for all ramps.

### D. Probabilistic Forecasting of Ramp Start-Time

In addition to the occurrence probability of ramp duration, the balancing authorities are also concerned with the probability of ramp start-time so as to prepare sufficient ancillary services, such as ramping reserves. Thus, we also calculate the probability of ramp start-time.

Fig. 7 illustrates the probability of up-ramp start-time. It is shown that both the first and the third up-ramps are successfully located into the time interval with a high occurrence probability. For instance, the first up-ramp starts during 27-28 hours with the highest probability, 95.16%, and the third up-ramp starts during 63-64 hours with a high probability, 89.52%. The start-time of critical up-ramps is also challenging to be accurately forecasted due to its high uncertainty. For instance, during the 1-2 and 19-20 hours, there should not be any ramps in actual wind power data. But for the simulation results, the occurrence probability is relatively high. This can be partially attributed to the incorrect ramp magnitudes resulted by the large forecasting errors.

### E. Forecasting Accuracy: Reliability and Sharpness

The reliability and sharpness metrics have been widely used to evaluate the probabilistic forecasting accuracy [17].

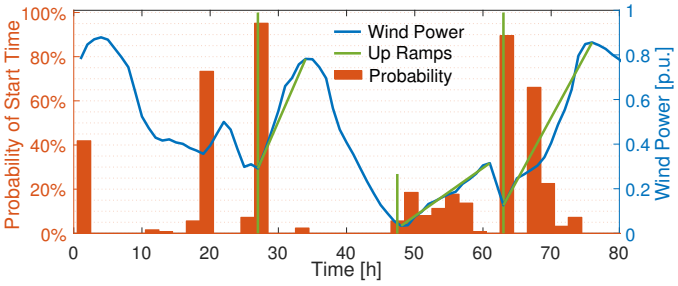


Fig. 7. Probabilistic forecast accuracy of up-ramp start-time.

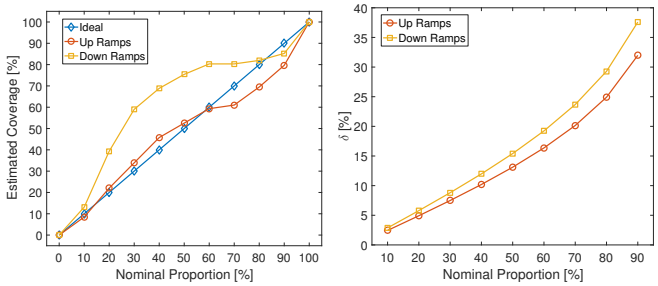


(a) Reliability (b) Sharpness

Fig. 8. Reliability and $\delta$-diagrams for evaluating the probabilistic ramp forecasting accuracy.

Reliability is the correct degree of a probabilistic forecasting assessed by the hit percentage. Sharpness is the uncertainty conveyed by the probabilistic forecasts estimated as the average interval size of different confident levels [18].

Fig. 8 compares the reliability and sharpness metrics for evaluating the probabilistic up- and down-ramp forecasting accuracy. The reliability of the probabilistic up-ramp forecast performs better than that of the probabilistic down-ramp forecast, since the estimated coverage curve of up-ramps converges closer to the ideal nominal proportion line (in blue). For the sharpness, both of the sharpness curves of the probabilistic up- and down-ramp forecasts are relatively low (under 40%). The probabilistic forecast of up-ramps shows a relatively lower sharpness than that of down-ramps.

## V. Conclusion

This paper developed a probabilistic wind power ramp forecasting method based on a large number of wind power forecasting scenarios. A deterministic wind power forecast was first generated by an ensemble machine learning model, and then used to calculate historical forecasting errors. A continuous Gaussian mixture model (GMM) was utilized to fit the probability distribution function (PDF) of wind power forecasting errors and to analytically deduce the corresponding cumulative distribution function (CDF). The inverse transform method based on the Monte Carlo sampling and CDF was used to generate the large number of forecasting error scenarios. An optimized swinging door algorithm was used to extract all the WPRs. Numerical results of a case study showed the effectiveness of the proposed method.

In the future, this research can be further improved by: (i) developing probabilistic wind power ramping products; and (ii) improving the probabilistic forecasting performance of critical wind power ramps.

## Acknowledgment

This work was supported by the National Renewable Energy Laboratory under Subcontract No. XGJ-6-62183-01 (under the U.S. Department of Energy Prime Contract No. DE-AC36-08GO28308).

## References

[1] Y. Qi and Y. Liu, "Wind power ramping control using competitive game," *IEEE Trans. Sustain. Energy*, vol. 7, no. 4, pp. 1516–1524, Oct. 2016.

[2] M. Cui, D. Ke, Y. Sun, D. Gan, J. Zhang, and B.-M. Hodge, "Wind power ramp event forecasting using a stochastic scenario generation method," *IEEE Trans. Sustain. Energy*, vol. 6, no. 2, pp. 422–433, Apr. 2015.

[3] Y. Liu, Y. Sun, D. Infield, Y. Zhao, S. Han, and J. Yan, "A hybrid forecasting method for wind power ramp based on Orthogonal Test and Support Vector Machine (OT-SVM)," *IEEE Trans. Sustain. Energy*, 2016, in press.

[4] N. Cutler, M. Kay, K. Jacka, and T. S. Nielsen, "Detecting categorizing and forecasting large ramps in wind farm power output using meteorological observations and WPPT," *Wind Energy*, vol. 10, no. 5, pp. 453–470, Sep. 2007.

[5] B. Greaves, J. Collins, J. Parkes, and A. Tindal, "Temporal forecast uncertainty for ramp events," *Wind Eng.*, vol. 33, no. 4, pp. 309–320, 2009.

[6] J. W. Taylor, "Probabilistic forecasting of wind power ramp events using autoregressive logit models," *European Journal of Operational Research*, 2016, in press.

[7] Y. Li, P. Musilek, E. Lozowski, C. Dai, T. Wang, and Z. Lu, "Temporal uncertainty of wind ramp predictions using probabilistic forecasting technique," in *2016 IEEE Second International Conference on Big Data Computing Service and Applications (BigDataService)*, Oxford, UK, 2016.

[8] A. Kaur, H. T. Pedro, and C. F. Coimbra, "Ensemble re-forecasting methods for enhanced power load prediction," *Energy Convers. Manag.*, vol. 80, pp. 582–590, 2014.

[9] D. Ke, C. Chung, and Y. Sun, "A novel probabilistic optimal power flow model with uncertain wind power generation described by customized gaussian mixture model," *IEEE Trans. Sustain. Energy*, vol. 7, no. 1, pp. 200–212, Jan. 2016.

[10] R. Singh, B. C. Pal, and R. A. Jabr, "Statistical representation of distribution system loads using gaussian mixture model," *IEEE Trans. Power Syst.*, vol. 25, no. 1, pp. 29–37, Feb. 2010.

[11] J. J. Moré and D. C. Sorensen, "Computing a trust region step," *SIAM J. Sci. Statist. Comput.*, vol. 4, no. 3, pp. 553–572, 1983.

[12] P. Glasserman, *Monte Carlo Methods in Financial Engineering*. New York, NY, USA: Springer, 2003.

[13] P. Pinson and R. Girard, "Evaluating the quality of scenarios of short-term wind power generation," *Appl. Energy*, vol. 96, pp. 12–20, 2012.

[14] M. Cui, J. Zhang, A. R. Florita, B.-M. Hodge, D. Ke, and Y. Sun, "An optimized swinging door algorithm for identifying wind ramping events," *IEEE Trans. Sustain. Energy*, vol. 7, no. 1, pp. 150–162, 2016.

[15] Y. Fu, M. Liu, and L. Li, "Multiobjective stochastic economic dispatch with variable wind generation using scenario-based decomposition and asynchronous block iteration," *IEEE Trans. Sustain. Energy*, vol. 7, no. 1, pp. 139–149, Jan. 2016.

[16] C. Draxl, A. Clifton, B.-M. Hodge, and J. McCaa, "The wind integration national dataset (WIND) Toolkit," *Appl. Energy*, vol. 151, pp. 355–366, 2015.

[17] P. Pinson, H. A. Nielsen, J. K. Møller, H. Madsen, and G. N. Kariniotakis, "Non-parametric probabilistic forecasts of wind power: required properties and evaluation," *Wind Energy*, vol. 10, no. 6, pp. 497–516, 2007.

[18] C. Gallego-Castillo, R. Bessa, L. Cavalcante, and O. Lopez-Garcia, "On-line quantile regression in the RKHS (Reproducing Kernel Hilbert Space) for operational probabilistic forecasting of wind power," *Energy*, vol. 113, pp. 355–365, 2016.